Robotica (1999) volume 17, pp. 437–445. Printed in the United Kingdom © 1999 Cambridge University Press

The Tricept robot: Inverse kinematics, manipulability analysis and closed-loop direct kinematics algorithm

Bruno Siciliano

PRISMA Lab, Dipartimento di Informatica e Sistemistica, Università degli Studi di Napoli Federico II, Via Claudio 21, 80125 Napoli (Italy)
E-mail: siciliano@disna.dis.unina.it

(Received in Final Form: March 17, 1999)

SUMMARY
This paper is aimed at presenting a study on the kinematics of the Tricept robot, which comprises a three-degree-of-freedom (dof) parallel structure having a radial link of variable length. The robot workspace is characterized and the inverse kinematics equation is obtained by using spherical coordinates. The inverse differential kinematics and statics are derived in terms of both an analytical and a geometric Jacobian, and a manipulability analysis along the various workspace directions is developed using the concept of force and velocity ellipsoids. A Jacobian-based Closed-Loop Direct Kinematics (CLDK) algorithm is presented to solve the direct kinematics problem along a given trajectory. Simulation results are illustrated for an industrial robot of the Tricept family.

KEYWORDS: Parallel robots; Inverse kinematics; Jacobian, Manipulability ellipsoids; Direct kinematics algorithms.

1. INTRODUCTION

Assembly workcells have long constistuted a typical field of application of industrial robots. Conventional open kinematic chain manipulators have been successfully used to perform assembly of electronic components, e.g. the SCARA robot. On the other hand, for assembly of mechanical or electromechanical parts, new robot manipulator geometries have been sought to achieve high position accuracy along with large payload capability. In this respect, the adoption of closed-chain mechanisms has constituted a breakthrough in the area. Robot manipulators with a parallelogram structure have been designed to naturally counterbalance the weight of the outer links of the kinematic chain.

Recently, a novel type of closed-chain manipulators have been receiving quite a deal of attention; namely, the parallel robots[1] which are constituted by a fixed base and a mobile base, connected by a number of independent kinematic chains. This allows obtaining high structural stiffness and performing high-speed motions, e.g. the Delta robot[2] and the Hexa robot.[3] One drawback with respect ot open-chain manipulators, though, is a typically reduced workspace. In the study of kinematics of parallel robots, the inverse kinematics problem admits an analytical solution whereas the direct kinematics problem may require the use of iterative algorithms.

A particular family of parallel robots is characterized by having a radial link connected to the end effector of variable length. To this family belongs the industrial robot Tricept HP1 integrated by Comau.[4] It is a six-degree-of-freedom (dof) robot manipulator comprising a three-dof parallel structure and a spherical wrist.

This work is aimed at studying the kinematics of this family of robots, with specific concern to the parallel structure. The robot workspace is characterized and spherical coordinates are used to obtain the inverse kinematics equation of the structure. Then, the inverse differential kinematics mapping is derived in terms of the inverse Jacobian, both the inverse analytic Jacobian and the inverse geometric Jacobian.[5] In force of duality, the inverse statics mapping is also derived. Such mappings are effectively used to perform a velocity and force analysis by means of manipulability ellipsoids,[6] demonstrating the features of the structure from a design standpoint.

The above Jacobians are at the basis of an algorithm to solve the direct kinematics problem which is developed by transposition of the well-known Closed-Loop Inverse Kinematics (CLIK) algorithm[7] used for open-chain robot manipulators. The algorithm can employ either the transpose of the inverse Jacobian or the direct Jacobian; in the former case, a simple Layapunov argument is used to prove algorithm convergence. For given joint motion trajectories, the resulting trajectory of the mobile base is computed in terms of both position and velocity. It should be mentioned that this type of algorithm has already been succesfully used for the Hexa robot.[8,9]

Simulation results are illustrated throughout the paper to validate the theoretical findings.

2. INVERSE KINEMATICS

Most spatial parallel robot prototypes are characterized by having the outer link connected to the end effector of variable length. Just recently, the adoption of parallel structures has found a fertile field also in the robotic industry. The Tricept HP1 integrated by Comau is a commercially available robot (Fig. 1), whose primary application is in the area of assembly when large insertion

https://doi.org/10.1017/S0263574799001678 Published online by Cambridge University Press

forces are required, e.g., as in the automobile industry. Other applications include deburring, milling, wood machining, laser and water-jet cutting, spot and laser welding. An International Parallel Kinematic Consortium has been recently established (October 1998) which is coordinated by Siemens[10] and gathers all the industrial partners engaged into the Tricept project.

The robot manipulator has a three-dof structure of parallel type to execute translational motions and a three-dof spherical wrist to execute rotational motions. The inventor of this structure is K.-E. Neumann[11] while the mechanics has been constructed by Neos.[12] The design has been logically derived from the Tetrabot.[13] Its workspace is to be considered quite large relative to the robot size, as can be appreciated from the two side views and the top view in Figure 2. In order to further enlarge the size of the workspace, the addition of a revolute joint at the fixed based has been envisaged, leading to kinematic redundancy into the robot manipulator.

As for the spherical wrist, this is standard and its direct and inverse kinematics is well known, see e.g., reference [5]. Hence, in the remainder the study will focus on the parallel structure only.

With reference to Figure 3, the parallel structure consists of three links with actuated prismatic joints (2) allowing translation along axis III. The fixed base (equilateral triangle) (1) is part of the supporting structure of the manipulator. Each link is connected to the triangle by means of a Cardan joint (3) allowing the link to rotate about axes I and II that are both orthogonal to the link. On the other end, the links are connected to the mobile base (equilateral triangle) (4) by three spherical joints (5). Besides the above three links, a radial link (6) is present: This is connected to the fixed base by a three-dof joint allowing the link to rotate about axes IV and V that are both orthogonal to the link, and to translate along through-hole axis VI; the connection of the radial link to the mobile base is fixed and orthogonal so as to avoid axial rotations and determine the reference point for the attachment of the spherical wrist.

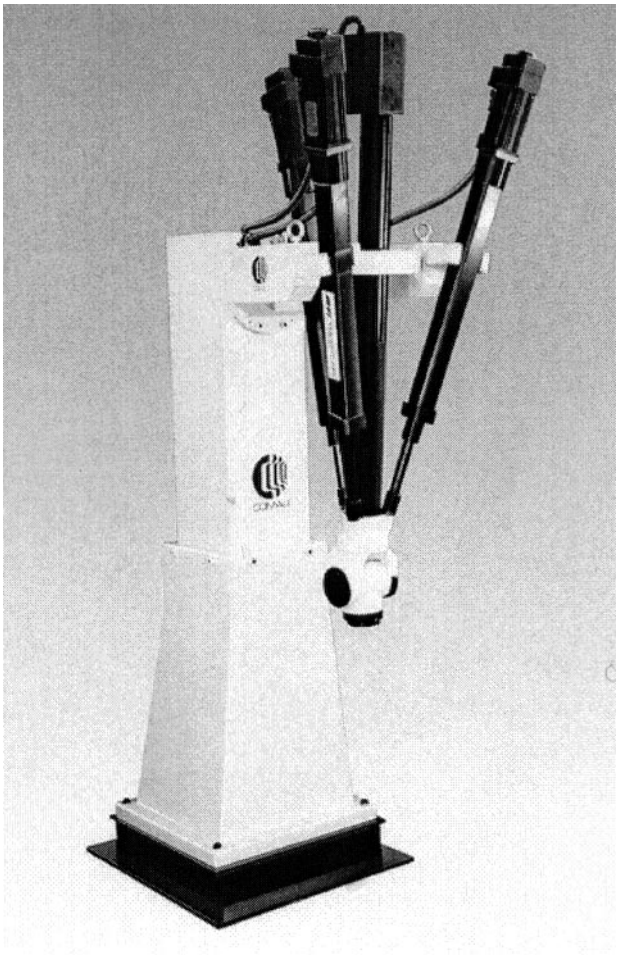

Fig. 1. The robot Comau Tricept HP1.

According to Grübler]s formula,[1] the structure is comprised of 8 bodies, 10 joints (3 spherical with 3 dof's each, 3 Cardan with 2 dof's each, 3 prismatic with 1 dof each, and 1 3-dof joint) and thus its mobility is $6\cdot(8-10-1)+3\cdot 3+3\cdot 2+31+3=3$, and thus the actuation of the 3 prismatic joints.

It is easy to recognize that the parallel structure has three dof's which are described by the axial translation of the radial link and by the two rotations about two axes orthogonal to the link itself. Consider the frame $O_0-x_0y_0z_0$ attached to the fixed base and the frame $O_3-x_3y_3z_3$ attached to the mobile base, and let r, α, β denote a set of spherical coordinates (Figure 4). With reference to the robot workspace, these coordinates vary within the limits

$$930\le r\le 1530 \qquad -\frac{\pi}{3}\le\alpha\le\frac{\pi}{3} \qquad -\frac{\pi}{3}\le\beta\le\frac{\pi}{3} \tag{1}$$

where dimensions are expressed in mm and rad; further, the side lengths of the two triangles are $a=600$ for the fixed base and $b=173$ for the mobile base, respectively.

The inverse kinematics equation gives the vector of prismatic joint variables $\boldsymbol{q}=[q_2\ q_2\ q_3]^T$ as a function of the vector of spherical coordinates $\boldsymbol{x}=[r\ \alpha\ \beta]^T$. In order to derive it, it is sufficient to consider the origin of frame 3 with respect to frame 0 described by the position vector

$$O_0O_3=\begin{bmatrix} x\\ y\\ z\end{bmatrix}=\begin{bmatrix} rs_\alpha c_\beta\\ rs_\beta\\ rc_\alpha c_\beta\end{bmatrix} \tag{2}$$

and the orientation of frame 3 with respect to frame 0 described by the rotation matrix

$$\boldsymbol{R}_3^0=\begin{bmatrix} c_\alpha & -s_\alpha s_\beta & s_\alpha\\ 0 & c_\beta & s_\beta\\ -s_\alpha & -c_\alpha s_\beta & c_\alpha c_\beta\end{bmatrix}, \tag{3}$$

where standard abbreviations $s_\alpha=\sin\alpha$, $c_\alpha=\cos\alpha$ have been used. Notice that the above transformation from spherical to Cartesian coordinates is always well defined except when $\beta=\pm\pi/2$ but, with reference to (1), this value is of no interest since it is outside the robot workspace.

After simple computation, the inverse kinematics equation can be obtained in the form:

https://doi.org/10.1017/S0263574799001678 Published online by Cambridge University Press

$$q_1^2 = \frac{1}{3}a^2 + \frac{1}{3}b^2 + r^2 - \frac{2}{3}abc_\alpha - \frac{2}{\sqrt{3}}ars_\alpha c_\beta$$

$$q_2^2 = \frac{1}{3}a^2 + \frac{1}{3}b^2 + r^2 - \frac{1}{2}ab\left(\frac{1}{3}c_\alpha + \frac{1}{\sqrt{3}}s_\alpha s_\beta + c_\beta\right)$$

$$+ar\left(\frac{1}{\sqrt{3}}s_\alpha c_\beta - s_\beta\right) \quad (4)$$

$$q_3^2 = \frac{1}{3}a^2 + \frac{1}{3}b^2 + r^2 - \frac{1}{2}ab\left(\frac{1}{3}c_\alpha - \frac{1}{\sqrt{3}}s_\alpha s_\beta + c_\beta\right)$$

$$+ar\left(\frac{1}{\sqrt{3}}s_\alpha c_\beta + s_\beta\right).$$

Notice that the solution is unique since the joint variables attain positive values only.

3. MANIPULABILITY ANALYSIS

Having determined the inverse kinematics equation, it is possible to compute the inverse differential kinematics mapping between the vector of task space velocities $\dot{\mathbf{x}} = [\dot{r}\ \dot{a}\ \dot{\beta}]^T$ and the vector of joint velocities $\dot{\boldsymbol{q}} = [\dot{q}_1\ \dot{q}_2\ \dot{q}_3\ ]^T$ in the form

$$\dot{\boldsymbol{q}} = \boldsymbol{J}_A^{-1}(x)\dot{x} \quad (5)$$

with

$$\boldsymbol{J}_A^{-1} = \begin{bmatrix} \frac{r - \frac{a}{\sqrt{3}}s_\alpha c_\beta}{q_1} & \frac{\frac{ab}{3}s_\alpha - \frac{ar}{\sqrt{3}}c_\alpha c_\beta}{q_1} & \frac{\frac{ar}{\sqrt{3}}s_\alpha s_\beta}{q_1} \\ \frac{2r + \frac{a}{\sqrt{3}}s_\alpha c_\beta - as_\beta}{2q_2} & \frac{\frac{ab}{6}s_\alpha - \frac{ab}{2\sqrt{3}}c_\alpha s_\beta + \frac{ar}{\sqrt{3}}c_\alpha c_\beta}{2q_2} & \frac{\frac{ab}{2}s_\beta - \frac{ab}{2\sqrt{3}}s_\alpha c_\beta - arc_\beta - \frac{ar}{\sqrt{3}}s_\alpha s_\beta}{2q_2} \\ \frac{2r + \frac{a}{\sqrt{3}}s_\alpha c_\beta + as_\beta}{2q_3} & \frac{\frac{ab}{6}s_\alpha + \frac{ab}{2\sqrt{3}}c_\alpha s_\beta + \frac{ar}{\sqrt{3}}c_\alpha c_\beta}{2q_3} & \frac{\frac{ab}{2}s_\beta + \frac{ab}{2\sqrt{3}}s_\alpha c_\beta + arc_\beta - \frac{ar}{\sqrt{3}}s_\alpha s_\beta}{2q_3} \end{bmatrix} \quad (6)$$

where, with reference to (4), the property $\dot{q}_i = (1/2q_i)(dq_i^2/dt)$ for $i = 1, 2, 3$ has been exploited. The matrix $\boldsymbol{J}_A$ is the analytical Jacobian[5] to be distinguished from the geometric Jacobian $\boldsymbol{J}$ relating the joint velocity vector to the linear velocity vector $\boldsymbol{v} = [v_x\ v_y\ v_z]^T$ obtained from the position vector $\boldsymbol{p} = [x\ y\ z]^T$ of the origin of the frame attached to the mobile base (Figure 4). The inverse differential kinematics in terms of the geometric Jacobian is written as

$$\dot{\boldsymbol{q}} = \boldsymbol{J}^{-1}(\boldsymbol{p})\boldsymbol{v}. \quad (7)$$

By comparing (5) with (7), the relationship between the two Jacobians is established by

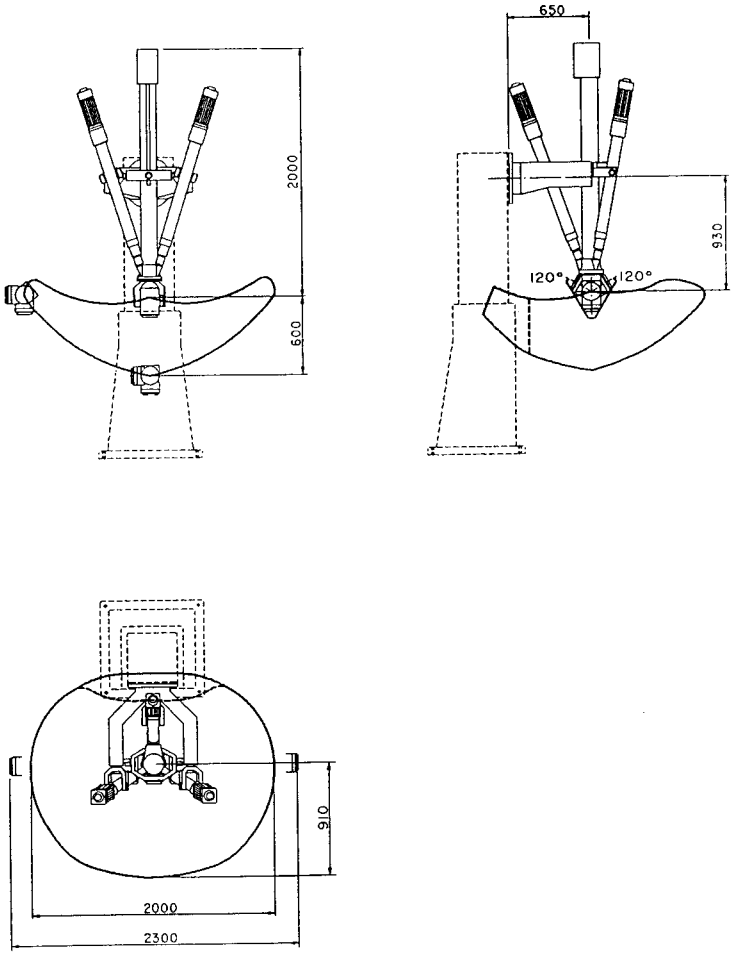

Fig. 2. Side and top views of robot workspace.

https://doi.org/10.1017/S0263574799001678 Published online by Cambridge University Press

$$\boldsymbol{J}^{-1}(\boldsymbol{p}) = \boldsymbol{J}_A^{-1}(\boldsymbol{x})\boldsymbol{T}_A(\boldsymbol{p}) \tag{8}$$

where the transformation matrix is

$$\boldsymbol{T}_A = \begin{bmatrix} \frac{x}{\sqrt{x^2+y^2+z^2}} & \frac{y}{\sqrt{x^2+y^2+z^2}} & \frac{z}{\sqrt{x^2+y^2+z^2}} \\ \frac{z}{x^2+z^2} & 0 & -\frac{x}{x^2+z^2} \\ -\frac{xy}{(x^2+y^2+z^2)\sqrt{x^2+z^2}} & \frac{x^2+z^2}{(x^2+y^2+z^2)\sqrt{x^2+z^2}} & \frac{yz}{-(x^2+y^2+z^2)\sqrt{x^2+z^2}} \end{bmatrix}. \tag{9}$$

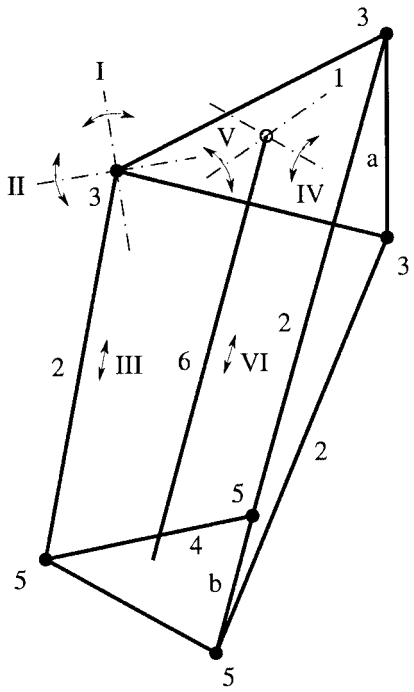

Fig. 3. Characterization of parallel structure.

The above workspace limits (1) can be expressed in terms of Cartesian coordinates as

$$-765\sqrt{3} \le x \le 765\sqrt{3} \quad -765\sqrt{3} \le y \le 765\sqrt{3} \quad 382.5 \le z \le 1530 \tag{10}$$

from which it can be seen that $\boldsymbol{T}_A$ is always nonsingular inside the workspace. In fact, as a result of a MATLAB simulation, Figure 5 illustrates the determinant of $\boldsymbol{T}_A$ as a function of x and y for $z=1000$. It can be seen that the transformation $\boldsymbol{T}_A$ does not introduce representation singularities, and the singularities of the inverse differential kinematics mapping are those of either $\boldsymbol{J}_A^{-1}$ or $\boldsymbol{J}^{-1}$. In particular, a singularity analysis of the determinant of $\boldsymbol{J}_A^{-1}$ reveals that this is always different from zero inside the workspace, e.g., as illustrated also in Figure 5 as a function of α and β for $r=1000$. The apparent discrepancy in the orders of magnitude of the two determinants in Figure 5 is just caused by the use of millimeters in the dimensions.

By virtue of the duality established by the principle of virtual works, the inverse statics mapping between the vector of joint torques τ and the vector of linear forces $\boldsymbol{f}$ on the mobile base is given by

$$\boldsymbol{f} = \boldsymbol{J}^{-\mathrm{T}}(\boldsymbol{p})\tau. \tag{11}$$

The kineto-static duality can be keenly exploited to carry out a velocity/force analysis of the structure in terms of manipulability ellipsoids.[6] The sphere in the joint velocity space

$$\dot{\boldsymbol{q}}^{\mathrm{T}}\dot{\boldsymbol{q}} = 1 \tag{12}$$

under the mapping (7) is transformed into the velocity manipulability ellipsoid in the linear velocity space

$$\boldsymbol{v}^{\mathrm{T}}(\boldsymbol{J}(\boldsymbol{p})\boldsymbol{J}^{\mathrm{T}}(\boldsymbol{p}))^{-1}\boldsymbol{v} = 1. \tag{13}$$

Dually, the sphere in the joint torque space

$$\tau^{\mathrm{T}}\tau = 1 \tag{14}$$

under the mapping (11) is transformed into the force manipulability ellipsoid in the linear force space

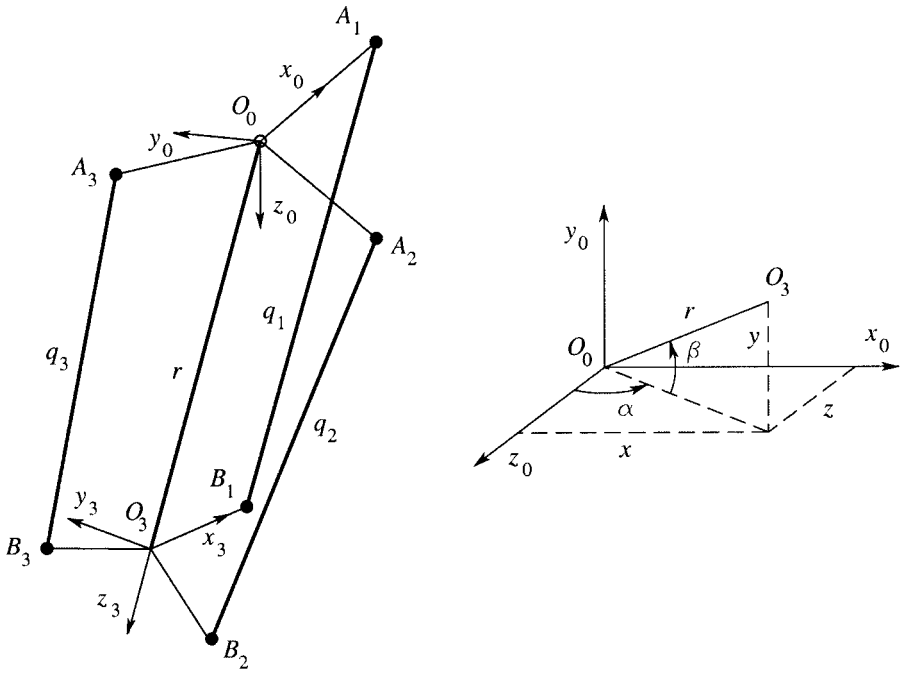

Fig. 4. Left: frame definitions – right: spherical and Cartesian coordinates.

https://doi.org/10.1017/S0263574799001678 Published online by Cambridge University Press

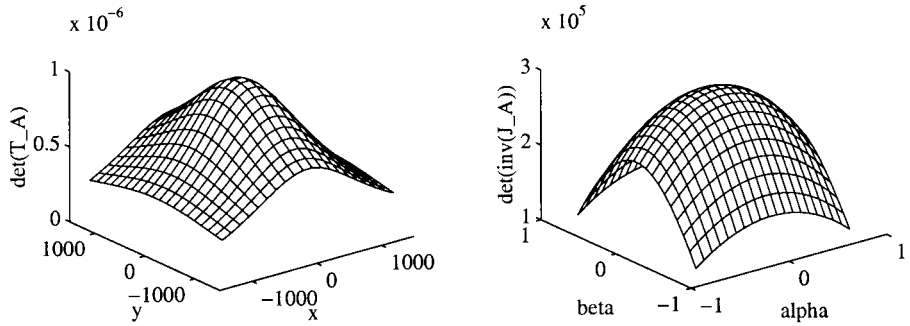

Fig. 5. Left: determinant of transformation matrix – right: determinant of inverse of analytical Jacobian.

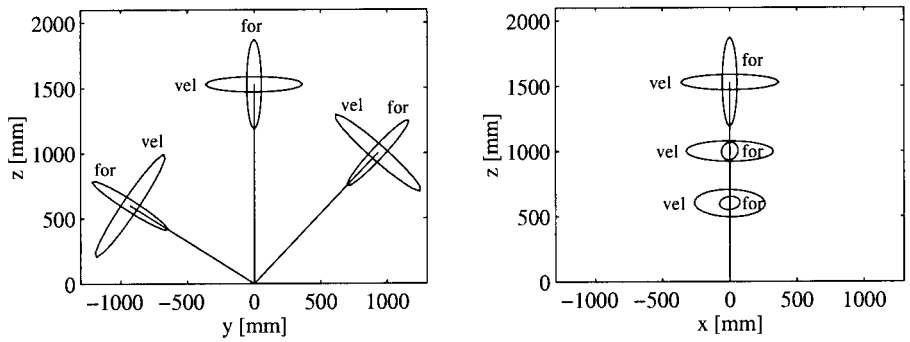

Fig. 6. Force and velocity manipulability ellipses. Left: in plane *yz* – right: in plane *xz*.

$$\boldsymbol{f}^{\mathrm{T}}(\boldsymbol{J}(\boldsymbol{p})\boldsymbol{J}^{\mathrm{T}}(\boldsymbol{p}))\boldsymbol{f}=1. \tag{15}$$

The principal axes of the two ellipsoids coincide, while the dimensions of the respective axes are in inverse proportion. Therefore, according to the concept of force/velocity duality, a direction along which good velocity manipulability is obtained is a direction along which poor force manipulability is obtained, and vice versa. This is confirmed by the results in Figure 6 which illustrate the intersections of the force and velocity manipulability ellipsoids with the *yz* plane and the *xz* plane, respectively, when the manipulator is in the following configurations: $\boldsymbol{p}=[0\ 0\ 1530]^{\mathrm{T}}$, $\boldsymbol{p}=[0\ -930\ 600]^{\mathrm{T}}$, $\boldsymbol{p}=[0\ 930\ 1000]^{\mathrm{T}}$.

Further insight into the robot manipulability can be gained by resorting to the mechanical transformer formalism in reference [14]. Once a unit vector $\boldsymbol{u}$ along a direction has been assigned, it is possible to compute the transformation ratio for the velocity manipulability ellipsoid as

$$\nu(\boldsymbol{p})=\left(\boldsymbol{u}^{\mathrm{T}}(\boldsymbol{J}(\boldsymbol{p})\boldsymbol{J}^{\mathrm{T}}(\boldsymbol{p}))^{-1}\boldsymbol{u}\right)^{-1/2} \tag{16}$$

and for the force manipulability ellipsoid as

$$\phi(\boldsymbol{p})=\left(\boldsymbol{u}^{\mathrm{T}}\boldsymbol{J}(\boldsymbol{p})\boldsymbol{J}^{\mathrm{T}}(\boldsymbol{p})\boldsymbol{u}\right)^{-1/2}. \tag{17}$$

The transformation ratios have been computed at certain robot configurations along given directions (see Table I). A comparison between the results in the first two rows clearly indicates the capability of the robot to exert larger values of forces along the vertical direction as well as to move at larger speeds along a horizontal direction. Also, from a comparison between the results in the first and third rows it is seen that ν increases while ϕ decreases as z decreases; this is in agreement with the fact, as z increases, the prismatic joints tend to attain a vertical configuration and thus they have a better capability to exert forces along that direction. Interestingly enough, at the configuration in the fourth to sixth row, the length of the radial link is equal to that in the configuration in the first two rows; the results in those rows confirm the intuition that the mechanical structure is designed so as to exhibit a good attitude to exert forces along the direction of the radial link, and such

Table I. Transformation ratios for certain configurations along given directions

$\boldsymbol{p}^{\mathrm{T}}$	$\boldsymbol{u}^{\mathrm{T}}$	ν	ϕ
[0 0 1530]	[0 0 1]	0.584	1.710
[0 0 1530]	[0 −1 0]	3.653	0.274
[0 0 1050]	[0 0 1]	0.593	1.686
[662.5 1325 382.5]	[0 0 1]	2.389	0.064
[662.5 1325 382.5]	[0 −1 0]	0.669	0.294
[662.5 1325 382.5]	[0.433 0.866 0.25]	0.583	1.633

https://doi.org/10.1017/S0263574799001678 Published online by Cambridge University Press

attitude improves as much as the radial link tends to be aligned with the vertical direction.

4. CLDK ALGORITHM

The direct kinematics problem for a parallel robot consists of finding the vector of position coordinates $\boldsymbol{p}$ (or $\boldsymbol{x}$) as a function of the vector of joint variables $\boldsymbol{q}$. Typically, such a problem does not admit closed-form solutions and numerical algorithms should be used. A crucial point with using a numerical algorithm[15] regards the possibility of computing all the feasible solutions to the problem, and preventing solutions to jump from one branch to another. For the parallel structure at issue in this work, up to eight solutions can be found; this result can be derived by referring to the direct kinematics of the parallel manipulator analyzed in reference [16] when three of the six links have fixed length and intersect at a common point.

A conceptually different approach to the problem can be pursued as follows. Instead of seeking one (or more) position solution corresponding to the given set of joint variable, the direct kinematics problem can be formulated as that to determine the motion of the mobile base as a function of the joint motion. In other words, assume that the initial joint configuration is assigned and a corresponding feasible position is known, e.g. via an off-line analytical or numerical procedure; assume, also, that a joint trajectory is assigned as a function of time (joint positions and velocities). Then, the goal is to compute on-line the resulting trajectory of the mobile base (position and velocity) starting from the initial posture of the robot. Such an approach involves the use of the robot differential kinematics as in the well-known Closed-Loop Inverse Kinematics (CLIK) scheme[7] developed for open-chain robot manipulators, which provides an inverse kinematics algorithm whose convergence is ensured through the stability of a closed-loop dynamic system of the tracking error.

Therefore, an effective solution to the direct kinematics problem for a parallel robot can be devised by transposing the above CLIK algorithm as explained below. Let $\boldsymbol{q}_d$ denote a set of desired joint variables and

$$\boldsymbol{e} = \boldsymbol{q}_d - \boldsymbol{q} \tag{18}$$

denote the error between $\boldsymbol{q}_d$ and the computed joint variables $\boldsymbol{q}$. Differentiating (18) with respect to time and accounting for (7) yields

$$\dot{\boldsymbol{e}} = \dot{\boldsymbol{q}}_d - \boldsymbol{J}^{-1}(\boldsymbol{p})\boldsymbol{v} \tag{19}$$

This error dynamics equation is at the basis of a Closed-Loop Direct Kinematics (CLDK) algorithm based on the geometric Jacobian. In particular, taking

$$\boldsymbol{v} = \boldsymbol{J}(\boldsymbol{p})(\dot{\boldsymbol{q}}_d + \boldsymbol{K}\boldsymbol{e}) \tag{20}$$

leads to the linear system

$$\dot{\boldsymbol{e}} + \boldsymbol{K}\boldsymbol{e} = \boldsymbol{0}, \tag{21}$$

and the choice of a positive definite (symmetric) matrix gain $\boldsymbol{K}$ guarantees that the error uniformly converges to zero, i.e. $\boldsymbol{p}$ that can be computed by integration of (20) is a solution to the direct kinematics problem. Notice that both position and velocity are obtained for given joint position and velocities; the closed loop on the tracking error of the algorithm guarantees convergence and eliminates the steady-state errors, as in typical open-loop resolved rate schemes instead. The resulting CLDK algorithm can be represented in block scheme form as in Figure 7 which shows that the inverse of the Jacobian inverse has to be computed besides the inverse kinematics function in the return path.

An alternative and computationally more efficient solution can be devised which avoids the inversion of the inverse geometric Jacobian to compute $\boldsymbol{J}$ in (20). In fact, the choice

$$\boldsymbol{v} = \boldsymbol{J}^{-\mathrm{T}}(\boldsymbol{p})\boldsymbol{K}\boldsymbol{e} \tag{22}$$

is based on the transpose of the inverse geometric Jacobian. In this case, convergence of the algorithm can be studied by considering the positive definite Lyapunov function

$$V = \frac{1}{2}\boldsymbol{e}^{\mathrm{T}}\boldsymbol{K}\boldsymbol{e}. \tag{23}$$

Taking the time derivative of (23) and computing it along the trajectories of the error system (19) gives

$$\dot{V} = \boldsymbol{e}^{\mathrm{T}}\boldsymbol{K}\dot{\boldsymbol{q}}_d - \boldsymbol{e}^{\mathrm{T}}\boldsymbol{K}\boldsymbol{J}^{-1}(\boldsymbol{p})\boldsymbol{J}^{-\mathrm{T}}(\boldsymbol{p})\boldsymbol{K}\boldsymbol{e} \tag{24}$$

which reveals that, if $\dot{\boldsymbol{q}}_d = \boldsymbol{0}$ then the second term is negative definite and thus $\boldsymbol{e}$ asymptotically converges to zero. On the other hand, for a time-varying trajectory $\dot{\boldsymbol{q}}_d \neq \boldsymbol{0}$, the tracking error can be upper bounded by suitably increasing the eigenvalues of $\boldsymbol{K}$ and in any case convergence is obtained at steady state. The resulting CLDK algorithm can be represented in block scheme form as in Figure 8 which

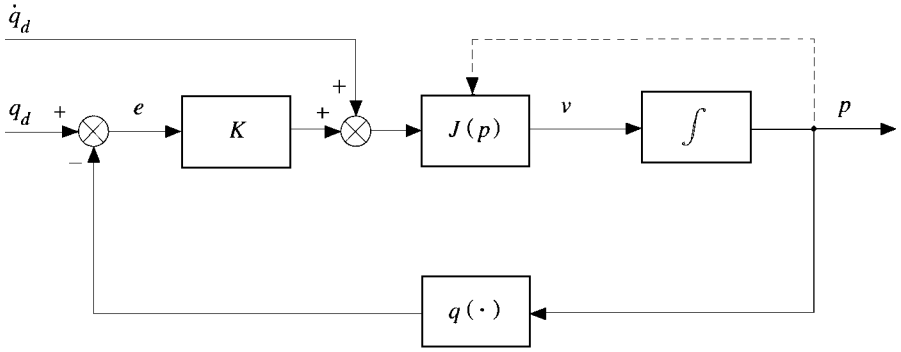

Fig. 7. Block scheme of CLDK algorithm using the inverse of the Jacobian inverse.

https://doi.org/10.1017/S0263574799001678 Published online by Cambridge University Press

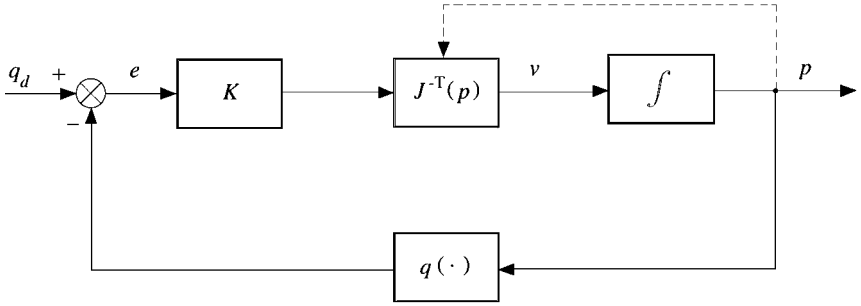

Fig. 8. Block scheme of CLDK algorithm using the transpose of the Jacobian inverse.

shows that the transpose of the Jacobian inverse has to be computed besides the inverse kinematics function in the return path. Notice that, differently from the solution (20), the solution (22) does not require the inversion of the inverse geometric Jacobian and thus it may work well also in the neighbourhood of kinematic singularities.

It should be clear that analogous direct kinematics algorithms can be formulated on the basis of the analytical Jacobian, and the expected performance is essentially the same as long as representation singularities are not encountered; as seen above, this is the case for the parallel robot at issue in this work.

In order to test the effectiveness of the presented direct kinematics algorithms, a case study has been simulated in MATLAB by using Euler numerical integration at 1 ms sampling time. The mobile base is in the initial position $\boldsymbol{p} = [0\ 0\ 1479.6]$ corresponding to the posture $\boldsymbol{q} = [1500\ 1500\ 1500]$. The following desired trajectory profile is assigned to the joint variables:

$$\boldsymbol{q}_d(t) = \begin{cases} \begin{bmatrix} 152t^3 - 456t^2 + 1500 \\ 165t^3 - 495t^2 + 1500 \\ 41t^3 - 123t^2 + 1500 \end{bmatrix} & 0 \le t \le 2 \\ \begin{bmatrix} 891 \\ 838 \\ 1337 \end{bmatrix} & t > 2. \end{cases}$$

The two algorithms based on solutions (20) and (22) have been implemented with a matrix gain $\boldsymbol{K} = \mathrm{diag}\{500, 500, 500\}$. The results are illustrated in Figures 9 and 10 in terms of the time history of the three components of position and velocity of the mobile base and of the norm of the tracking

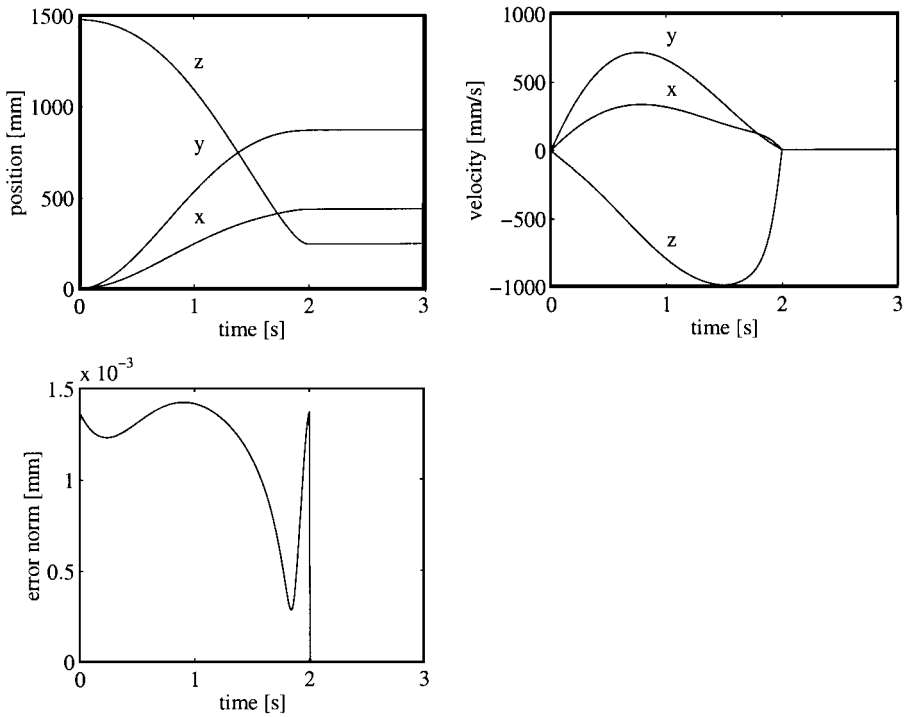

Fig. 9. Time history of position and velocity of mobile base and norm of tracking error for the CLDK algorithm based on the inverse of the Jacobian inverse.

https://doi.org/10.1017/S0263574799001678 Published online by Cambridge University Press

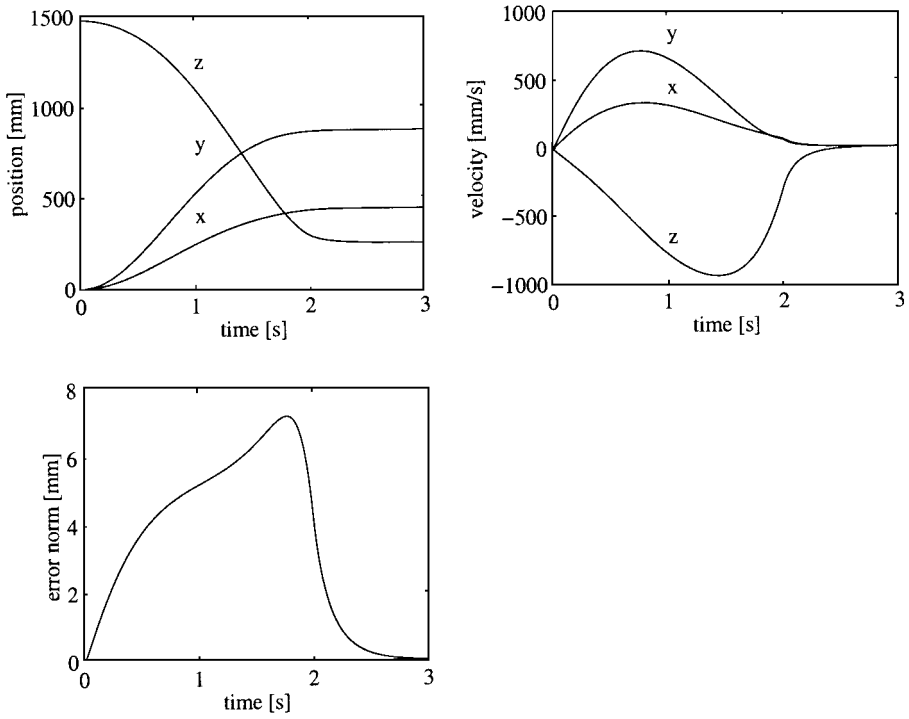

Fig. 10. Time history of position and velocity of mobile base and norm of tracking error for the CLDK algorithm based on the transpose of the Jacobian inverse.

error, for the two algorithms, respectively. It can be recognized that the tracking error is practically null for the first algorithm, and is anyhow limited for the second algorithm (of the order of the millimeter). Nevertheless, error convergence to zero at steady state is ensured in both cases. Furthermore, it can be recognized how the resulting motion of the mobile base is continuous, i.e. it does not involve any abrupt jump from one solution to another.

5. CONCLUSION

The results of a study on the kinematics of the Tricept parallel robot have been reported in this work. The inverse kinematics equation has been obtained in analytical form and the inverse Jacobian has been derived to characterize the inverse differential kinematics mapping. Based on a kineto-static duality concept, a manipulability analysis of the structure has been accomplished to ascertain the procedure to execute forces/velocities along given work-space directions. The direct kinematics problem has been solved by resorting to a closed-loop algorithm based either on the inverse or on the transpose of the inverse Jacobian, leading to computing both the position and velocity of the mobile base as a function of the joint trajectories. Simulation results for the industrial parallel robot Comau Tricept HP1 have shown the effectiveness of the approach.

ACKNOWLEDGEMENTS

This paper is partly based on previous work.[17] The work was supported by *Ministero dell'Università e della Ricerca Scientifica e Tecnologica* and by *Agenzia Spaziale Italiana*. The author would like to acknowledge valuable advice on the topic of parallel robots and useful comments on the contents of this paper by Jean-Pierre Merlet and François Pierrot, as well as by the anonymous reviewers.

References

1. J.-P. Merlet, *Les Robots Parallèles* (Hèrmes, Paris, France, 1990).
2. R. Clavel, "Delta, a fast robot with parallel geometry", *Proc. 18th Int. Symp. on Industrial Robots*, Lausanne, Switzerland (1988) pp. 91–100.
3. F. Pierrot, A. Fournier and P. Dauchez, "Towards a fully-parallel 6 dof robot for high-speed applications', *Proc. 1991 IEEE Int. Conf. on Robotics and Automation*, Sacramento, CA (1991) p. 1288–1293.
4. A. Baroncelli, "Il robot fa carriera" (in Italian), *Automazione e Robotica*, **14**, (Oct., 1996).
5. L. Sciavicco and B. Siciliano, *Modeling and Control of Robot Manipulators*, (McGraw-Hill, New York, NY, 1996).
6. T. Yoshikawa, "Manipulability of robotic mechanisms", *Int. J. Robotics Research* **4**, No. 1, 3–9 (1985).
7. B. Siciliano, "A closed-loop inverse kinematic scheme for on-line joint-based robot control", *Robotica* **8**, Part 3, 231–243 (1990).
8. Ph. Bégon, "Commande des Robots Parallèles Rapides. Application au Robot HEXA (in French)", *Thèse de Doctorat*, (Université Montpellier II, June 1995).
9. F. Pierrot, Ph. Bégon and P. Dauchez, "Control of fast parallel robots: Application to the HEXA robot", *Proc. Int. Symp. on Microsystems, Intelligent Materials and Robots*, Sendai, Japan (1995), pp. 572–575.
10. *International Parallel Kinematic Consortium*, Home page at http://www.ad.siemens.de/sinumerik/html_76/parakine/parakons.htm
11. K.-E. Neumann, *Robot* (US Patent 4,732,525, Neos Product HB, Norrtalje, Sweden, 1988).
12. *Neos Robotics*, Home page at http://www.neosrobotics.com/
13. G.S. Thornton, "The GEC Tetrabot – A new series-parallel assembly robot", *Proc. 1988 IEEE Int. Conf. on Robotics and Automation*, Philadelphia, PA (1988) pp. 437–439.
14. S.L. Chiu, "Task compatibility of manipulator postures", *Int. J. Robotics Research* **7**, No. 5, 13–21 (1988).

https://doi.org/10.1017/S0263574799001678 Published online by Cambridge University Press

15. O. Chételat, J.-P. Merlet, P. Myszkorowski and R. Longchamp, "Globally convergent iterative algorithm for coordinate transformations in articulated mechanisms", *Prepr. 5th IFAC Symp. on Robot Control*, Nantes, France (1997) pp. 743–749.
16. C. Innocenti and V. Parenti Castelli, "Direct kinematics of the 6–4 fully parallel manipulator with position and orientation uncoupled", *Proc. Euro. Robotics and Intelligent Systems Conf.* Corfou, Greece (1991).
17. B. Siciliano, "A study on the kinematics of a class of parallel manipulators", **In:** *Advances in Robot Kinematics: Analysis and Control* (J. Lenarčič and M.L. Husty, (Eds.) (Kluwer Academic Publishers, Dordrecht, The Netherlands (1998) pp. 29–38.

https://doi.org/10.1017/S0263574799001678 Published online by Cambridge University Press